The Plant Cell, Vol. 20: 1760–1774, July 2008, www.plantcell.org

Auxin Regulates *Arabidopsis* Anther Dehiscence, Pollen Maturation, and Filament Elongation [W]

Valentina Cecchetti,[a] Maria Maddalena Altamura,[b] Giuseppina Falasca,[b] Paolo Costantino,[a] and Maura Cardarelli[c,1]

[a] Dipartimento di Genetica e Biologia Molecolare, Istituto Pasteur Fondazione Cenci Bolognetti, Università La Sapienza, 00185 Rome, Italy

[b] Dipartimento di Biologia Vegetale, Università La Sapienza, 00185, Rome, Italy

[c] Istituto Biologia e Patologia Molecolari, Consiglio Nazionale delle Ricerche, Dipartimento di Genetica e Biologia Molecolare, Università La Sapienza, 00185 Rome, Italy

We provide evidence on the localization, synthesis, transport, and effects of auxin on the processes occurring late in *Arabidopsis thaliana* stamen development: anther dehiscence, pollen maturation, and preanthesis filament elongation. Expression of auxin-sensitive reporter constructs suggests that auxin effects begin in anthers between the end of meiosis and the bilocular stage in the somatic tissues involved in the first step of dehiscence as well as in the microspores and in the junction region between anther and filament. In situ hybridizations of the auxin biosynthetic genes *YUC2* and *YUC6* suggest that auxin is synthesized in anthers. In agreement with the timing of auxin effects, the *TIR1*, *AFB1*, *AFB2*, and *AFB3* auxin receptor-encoding genes are transcribed in anthers only during late stages of development starting at the end of meiosis. We found that in *tir1 afb* triple and quadruple mutants, anther dehiscence and pollen maturation occur earlier than in the wild type, causing the release of mature pollen grains before the completion of filament elongation. We also assessed the contribution of auxin transport to late stamen developmental processes. Our results suggest that auxin synthesized in anthers plays a major role in coordinating anther dehiscence and pollen maturation, while auxin transport contributes to the independent regulation of preanthesis filament elongation.

INTRODUCTION

In autogamous plants, three processes occurring late in stamen development contribute to a successful pollination at anthesis: anther dehiscence, necessary to release pollen on the stigma upon filament elongation; pollen maturation, allowing deposition on the stigma of pollen grains capable of germinating and thus reaching the ovules; and elongation of the stamen filament (preanthesis filament elongation), bringing the anthers close to the stigma. Hormones regulate these developmental processes and coordinate them with one another and with the development of the carpel. It has been demonstrated that jasmonic acid (JA) is involved in the final stages of anther dehiscence and pollen maturation and in filament elongation (Sanders et al., 2000; Ishiguro et al., 2001; Nagpal et al., 2005). In addition, it has been proposed that JA coordinates the release of pollen with the opening of the flower bud (Ishiguro et al., 2001).

Auxin-induced reporter activity was observed in anthers at late stages of development (Aloni et al., 2006; Feng et al., 2006), and *YUC* genes, responsible for auxin biosynthesis and encoding flavin monoxygenase, are expressed in developing stamens (Cheng et al., 2006).

[1] Address correspondence to maura.cardarelli@uniroma1.it.
The author responsible for distribution of materials integral to the findings presented in this article in accordance with the policy described in the Instructions for Authors (www.plantcell.org) is: Maura Cardarelli (maura.cardarelli@uniroma1.it).
[W] Online version contains Web-only data.
www.plantcell.org/cgi/doi/10.1105/tpc.107.057570

Auxin has been shown to regulate early stages of stamen development (Okada et al., 1991; Nemhauser et al., 2000; Cheng et al., 2006), and scattered evidence suggests that this hormone may also be involved in late developmental stages: in a previous work, we provided indirect evidence that auxin may regulate anther dehiscence, pollen development, and filament elongation in tobacco (*Nicotiana tabacum*; Cecchetti et al., 2004). In the auxin biosynthesis-defective *yuc2 yuc6* double mutants, stamens are formed, but subsequent stamen development is halted: anthers rarely produce any pollen, and stamens fail to elongate (Cheng et al., 2006). The involvement of auxin in late stamen development has also been suggested by the observation that double null mutants of the auxin response factors ARF6 and ARF8 have flowers with indehiscent anthers and short filaments (Nagpal et al., 2005) and that plants overexpressing the miR167 microRNA and showing reduced levels of *ARF6* and *ARF8* transcripts are defective in anther dehiscence, pollen germination, and filament elongation (Ru et al., 2006; Wu et al., 2006).

Additional indirect evidence comes from a study by Yassuor et al. (2006) on cotton (*Gossypium hirsutum*) and *Arabidopsis thaliana* flowers treated with the herbicide glyphosate. This treatment induced the accumulation of high levels of indole-3-acetic acid, and flowers exhibited delayed anther dehiscence due to changes in cell wall lignification of endothecium cells (Yassuor et al., 2006).

This study was designed to confirm and extend our previous suggestion that auxin plays a key role in regulating the late stages of stamen development (Cecchetti et al., 2004). Here, we show

that auxin coordinates anther dehiscence and pollen maturation as well as independently regulating filament elongation.

RESULTS

DR5 Promoter Activity Builds Up at the End of Meiosis in Tissues Involved in Anther Dehiscence, Pollen Maturation, and Filament Elongation

Late stamen developmental processes (anther dehiscence, pollen maturation, and preanthesis filament elongation) start in anthers after the end of meiosis (stage 10) and are completed at anthesis (stage 13) (for a description of the developmental stages of the *Arabidopsis* flower, see Bowman, 1994, and Figure 9 of this work).

To obtain information on the distribution of auxin in tissues involved in late stamen developmental processes, we analyzed *Arabidopsis* lines harboring the β-glucuronidase (GUS) and the green fluorescent protein (GFP) reporter genes driven by the auxin-inducible DR5 promoter (Ulmasov et al., 1997). *DR5:GUS* activity has been observed in anthers at late stages of development (Aloni et al., 2006; Feng et al., 2006), but a detailed tissue-specific analysis has not been provided.

Intense GUS-specific staining was observed in anthers of *DR5:GUS* plants at flower stages 10 through 11 (Figure 1A) but not at previous or subsequent stages of development. Figure 1B shows a *DR5:GUS* flower bud containing both unstained anthers in long stamens (at stage 12) and stained anthers in shorter stamens (at stage 11), as short stamens show a delayed development (Figure 1C). Tissue-specific localization of GUS-specific staining was analyzed in greater detail in transverse sections of *DR5:GUS* anthers. In *Arabidopsis*, tissues surrounding the theca (tapetum, middle layer, and endothecium) are involved in the first step of the anther dehiscence program that ends at stage 12 when septum lysis occurs. At the same stage, microspores complete the first mitotic division and the first (slow) phase of preanthesis filament elongation is completed (Bowman, 1994; this work). As shown in Figure 1D, GUS staining was not detectable in anthers during microsporogenesis (stage 9). It became intense at the end of meiosis (late stage 10) in tissues surrounding the theca, in microspores, and in the procambium of the anther and of the upper filament (anther-filament procambium) (Figures 1E to 1G). At late stage 11 (Figures 1H and 1I), GUS staining declined and was detectable only in the remnants of the middle layer, in the tapetum undergoing degeneration, in immature pollen grains, and in the anther-filament procambium. No GUS staining was observed in anthers when the septum degenerated and the anthers became bilocular (stage 12, Figures 1J and 1K).

As shown in Figures 1L to 1Q, the same inferences on the developmental pattern of auxin localization were derived from the analysis of *DR5:GFP* inflorescences, where GFP fluorescence was detected in all tissues described above, mainly in the junction region between anther and filament (Figures 1L and 1M), in tapetum cells (Figures 1M and 1N), and barely in pollen grains (Figure 1N). In addition, fluorescence was also intense at the tip of the anther (Figure 1O) at the tetrad stage (Figure 1P) as well as in the apex of the pistil (Figure 1Q). Thus, the activity of the DR5 promoter peaks in a developmental window that spans the microspore stage before the beginning of late developmental processes (stage 10), declines when pollen maturation and anther dehiscence processes begin (stage 11), and is no longer detectable when septum lysis occurs and tapetum degeneration is completed (stage 12).

To provide support to the notion that the activity of the DR5 promoter reflects auxin activity in developing stamens, *DR5:GUS* inflorescences were treated with exogenous auxin either in planta or in vitro. For the in planta treatment, plants were locally sprayed on inflorescences with 50 μM 1-naphthalene acetic acid (NAA) or with water. As in untreated *DR5:GUS* flowers described above (Figure 1A), GUS activity in water-treated inflorescences was detectable in anthers only at stages 10 and 11 (see Supplemental Figure 1A online). By contrast, in stamens of NAA-treated inflorescences, GUS staining was clearly detectable also at stages 12 and 13 (Figures 1R and 1S), mainly localized in the junction region between anther and filament and, to a lesser extent, in the filament (Figure 1S).

For the in vitro treatment, inflorescences excised from *DR5:GUS* plants were incubated 24 h in the presence of 50 μM NAA (or water) and analyzed for GUS activity. As shown in Supplemental Figure 1B online, in vitro water-treated inflorescences showed GUS staining in stamens only at stages 10 and 11, indistinguishable from that of untreated and in planta water-treated *DR5:GUS* inflorescences. By contrast, in vitro NAA-treated inflorescences showed intense staining in stamens also at stages 13 and 12, as shown in Figures 1T and 1U, respectively, localized (though more intense) as in planta treated inflorescences.

Auxin Biosynthetic Genes Are Active in Anther Tissues

To seek evidence that auxin is synthesized in the anther tissues where we observed DR5 activity, we analyzed the localization of the transcripts of the auxin biosynthetic genes *YUC2* and *YUC6* (Cheng et al., 2006). *YUC* gene expression in stamens had been previously shown by means of GUS constructs (Cheng et al., 2006), but no information about tissue specificity during stamen development was provided. Here, we analyzed the tissue-specific expression of *YUC2* and *YUC6* during stamen development by means of in situ mRNA hybridizations on longitudinal and transverse sections of stamens at stages 8 to 12. Control hybridizations are shown in Supplemental Figure 2 online.

As shown in Figure 2A, at premeiotic stage 8, *YUC2* mRNA was localized essentially in the thecas of the anther. At stage 9, the hybridization signal was very strong in the tapetum, in the middle layer, in the endothecium, in meiocytes, and in the procambium (Figure 2B). Later in development (late stage 9), just before auxin peaks at stages 10 to 11, as visualized through the activity of the DR5 promoter described above, the *YUC2* mRNA signal was very strong in the tetrads, in the tissues surrounding the theca, in the procambium of the anther (Figure 2C), and in the filament, in both procambium and epidermis (Figure 2D). At stage 10, when microspores are released, the *YUC2* mRNA hybridization signal decreased in all tissues surrounding the theca and in the microspores (Figure 2E) but not in the procambium. Later in

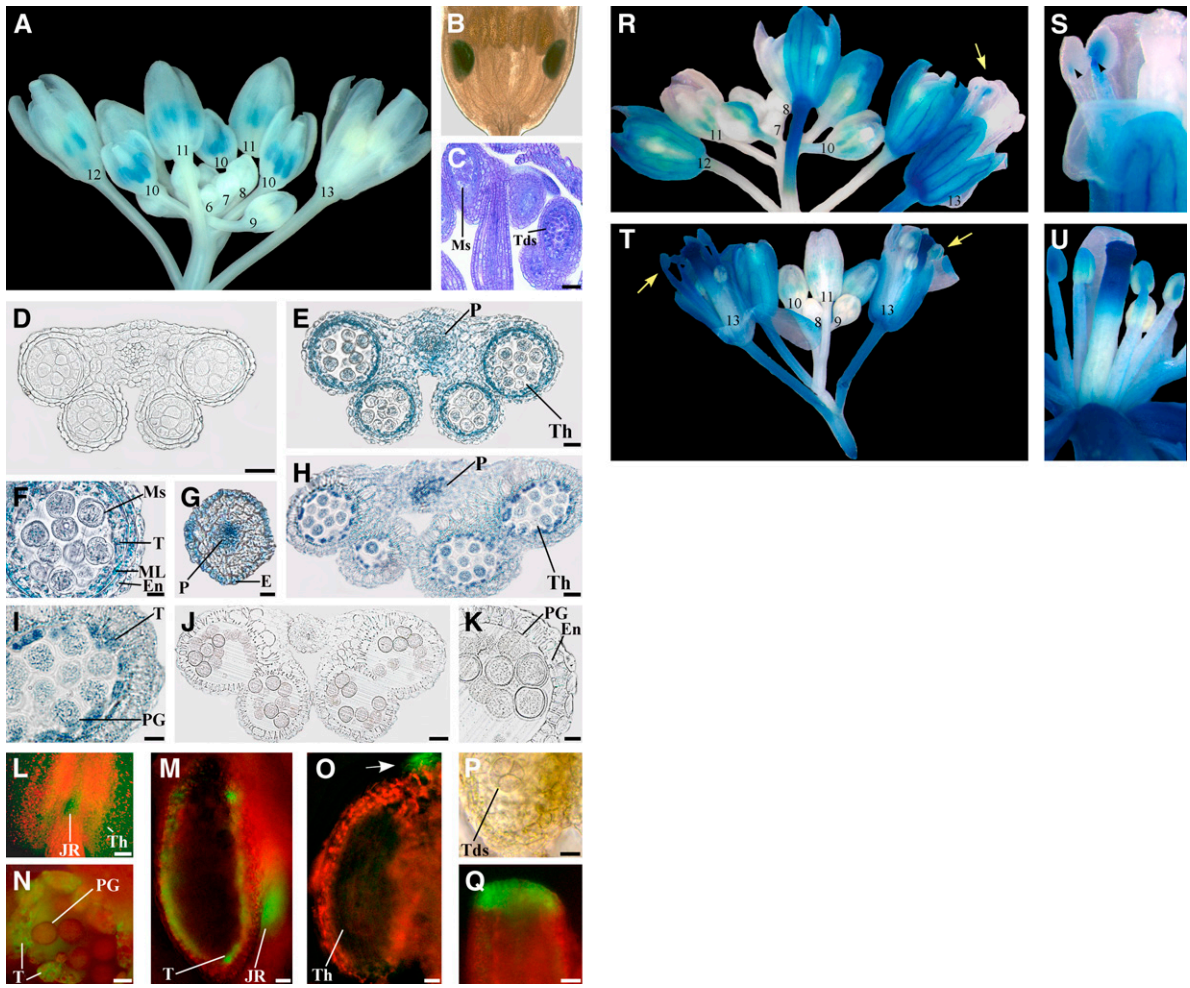

Figure 1. Auxin-Responsive Reporter Genes Are Transcribed in Anthers before the Onset of Late Developmental Programs and Are Induced by Exogenous Auxin.

(A) to **(C)** Expression of the *DR5:GUS* auxin-responsive reporter in flowers at different developmental stages.
(A) *DR5:GUS* inflorescence showing no GUS staining in flower buds at early stages of development (6 to 9), intense GUS staining (blue) in anthers at stages 10 and 11, GUS staining at stage 12 only in short stamens, and no GUS staining at stage 13. Numbers indicate flower developmental stages.
(B) *DR5:GUS* flower bud at early stage 12: GUS staining is observed in the anthers of short stamens.
(C) Longitudinal section of a *DR5:GUS* flower bud at stage 10: microspores are visible in the anthers of long stamens, whereas tetrads are visible in those of short stamens. Bar = 30 μm.
(D) to **(K)** Histochemical analysis of anthers in transection of *DR5:GUS* stamens.
(D) Anther at stage 9. GUS staining is absent at the onset of meiosis. Bar = 20 μm.
(E) Anther at late stage 10. Strong GUS staining at the end of meiosis in the theca and procambium. Bar = 20 μm.
(F) Detail of **(E)**. Strong GUS staining in the tapetum, middle layer, endothecium, and in microspores. Bar = 10 μm.
(G) Upper stamen filament at late stage 10: transverse section at the end of meiosis showing intense GUS staining in the procambium and epidermal cells. Bar = 20 μm.
(H) Anther at stage 11. GUS staining is observed in the theca and procambium. Bar = 20 μm.
(I) Detail of **(H)**. GUS signal is localized in tapetum degenerating cells and in pollen grains. Bar = 10 μm.
(J) Anther at stage 12. GUS staining is absent after septum lysis (bilocular anther). Bar = 30 μm.
(K) Detail of **(J)**. GUS signal is absent in the endothecium and pollen grains. Bar = 10 μm.
(L) to **(Q)** Fluorescence and bright-light images of anthers and pistils of *DR5:GFP* auxin-responsive reporter at different developmental stages.
(L) Stamen at late stage 10. GFP fluorescence (green) is visible in the theca and in the junction region between anther and filament. Bar = 80 μm.
(M) Stamen at late stage 11. Hand-cut longitudinal section showing intense GFP fluorescence in the remnants of the tapetum and in the junction region between anther and filament. Bar = 20 μm.
(N) Anther theca at late stage 11. Hand-cut transverse section showing intense GFP fluorescence in tapetum degenerating cells and faint fluorescence in pollen grains. Bar = 10 μm.
(O) to **(Q)** Anther and pistil at late stage 9.

development (late stage 11), *YUC2* mRNA was detectable mainly in the procambium (Figure 2F) where it was no longer detectable at stage 12 (Figure 2G). The *YUC6* mRNA was detected in the same anther tissues and stages as *YUC2*: stages 8, late 9, 10, and 12 are reported in Figures 2H to 2K, respectively. These results show that auxin biosynthetic genes are actively transcribed in tissues surrounding the thecas, in microspores, and in the procambium before the DR5 promoter is activated, and their transcription ceases in most of these tissues (except the procambium) prior to the observed decline in DR5 activity.

Severing and NPA Treatment Do Not Significantly Alter DR5 Promoter Activity in Anthers

To assess the possible contribution of transport of auxin through the filament to anthers, we severed anthers from *DR5:GUS* flower buds at the premeiotic stage (stage 8) and cultured anthers and flower buds in vitro. During culture, development of anthers progressed, and after 24 h (corresponding to stage 10 in planta) 50% of them showed microspore formation. As shown in Figure 3, while no GUS activity was detected in any anther before culture (Figure 3A), after 24 h ~50% of the flower buds showed intense GUS activity localized in the anthers (Figure 3B). All anthers severed from these buds exhibited a comparably intense DR5-driven GUS activity (Figure 3C), suggesting that auxin transport from the filament does not provide a major contribution to DR5 activation.

To further strengthen this point, immature inflorescences of *DR5:GUS* plants were sprayed in planta with either 10 or 100 μM 1-naphthylphthalamic acid (NPA), an auxin transport inhibitor, and GUS staining performed 24 h after treatment. GUS activity and localization was comparable in water-treated controls (Figures 3D and 3G) and in anthers treated with 10 μM NPA (Figures 3E and 3F) or 100 μM NPA (Figures 3H and 3I) (i.e, only stage 10-11 flowers showed GUS staining). These flowers were at meiotic or premeiotic stages (9 or earlier) at the time of treatment, indicating that a block of auxin transport at early stages of flower development had no major effect on DR5 activity in anthers.

Phenotypic analysis of in planta–treated inflorescences was performed at different times after spraying to allow the progressive maturation of the flower buds that were at different stages of development when inflorescences were treated. Stamen filament length was measured at stage 13, and anther dehiscence checked between stages 11 and 13.

Flowers that were at stages 12 and 11 at the time of treatment reached stage 13 after 24 and 48 h, respectively. Of these, flowers treated with either concentration of NPA had filaments that were 10% shorter than water-treated controls. At 24 h, the average (±SE) filament length was 1.67 ± 0.025 mm ($P < 0.01$), 1.69 ± 0.017 mm ($P < 0.01$), and 1.84 ± 0.019 mm in flowers treated with 10 μM NPA, 100 μM NPA, and water, respectively. At 48 h, the values were 1.66 ± 0.03 mm ($P < 0.01$), 1.70 ± 0.02 mm ($P < 0.01$), and 1.81 ± 0.03 mm, respectively. At 72 h and later, stage 13 was reached by flowers that were at early stages of development (10 or earlier) when treated, and the differences in filament lengths between NPA-treated flowers and controls were progressively smaller.

Analysis of anthers performed 24 h after NPA treatment showed that all anthers were dehiscent at stage 13 both in NPA-treated flowers and controls. By contrast, after 48 h, while all stage 13 anthers of water-treated flowers were dehiscent (Figure 3J), ~15 to 20% of the NPA-treated flowers showed indehiscent anthers at stage 13 (Figures 3K and 3L). At 72 h and later, no difference between controls and NPA-treated flowers was observed and all stage 13 anthers were dehiscent. This suggests that NPA is effective only when applied to flowers at stage 11 (i.e., late but before tapetum degeneration, as discussed below). No precocious dehiscence was observed in any NPA-treated flower.

The *TIR1*, *AFB1*, *AFB2*, and *AFB3* Genes Are Transcribed during Late Stamen Development

The results described in the previous sections suggest that auxin plays a role in late processes of stamen development. To assess whether the auxin receptor genes *TIR1*, *AFB1*, *AFB2*, and *AFB3* are expressed in late stamen development and whether their expression patterns are compatible with the above-described patterns of *YUC* expression and DR5 activity, reporter lines *TIR1:GUS*, *AFB1:GUS*, *AFB2:GUS*, and *AFB3:GUS* (Dharmasiri et al., 2005) were analyzed. As shown in Figures 4A1 to 4D1, at early stages of flower development (stages 8 to 9), no GUS-specific

Figure 1. (continued).

(O) Anther theca in longitudinal section showing GFP fluorescence at the tip of the anther (arrow) but not in the theca. Bar = 10 μm.
(P) Detail of **(O)** in bright light showing tetrads. Bar = 10 μm.
(Q) Detail of the apical region of the pistil. GFP fluorescence is intense in cells differentiating the papillae. Bar = 20 μm.
(R) to **(U)** Expression of the *DR5:GUS* reporter after 10 mM NAA treatment of in planta inflorescences (**[R]** and **[S]**) or excised inflorescences (**[T]** and **[U]**).
(R) *DR5:GUS* inflorescence showing no GUS staining in flower buds at early stages of development (7 and 8), intense GUS staining in anthers at stages 10 and 11, and GUS staining in stamens at stage 13 (arrow). Numbers indicate flower developmental stages.
(S) Detail of **(R)** flower at stage 13: GUS signal is observed in filaments and in the junction region between anther and filament (arrowheads).
(T) *DR5:GUS* inflorescence showing no GUS staining in flower buds at early stages of development (8 and 9), intense GUS staining in anthers at stages 10 and 11, and intense GUS staining in stamens at stage 13 (arrows). Numbers indicate flower developmental stages.
(U) *DR5:GUS* flower at late stage 12: GUS signal is observed in filaments and anthers.
E, epidermal cells; En, endothecium; JR, junction region; ML, middle layer; Ms, microspores; P, procambium; PG, pollen grains; T, tapetum; Tds, tetrads; Th, theca.

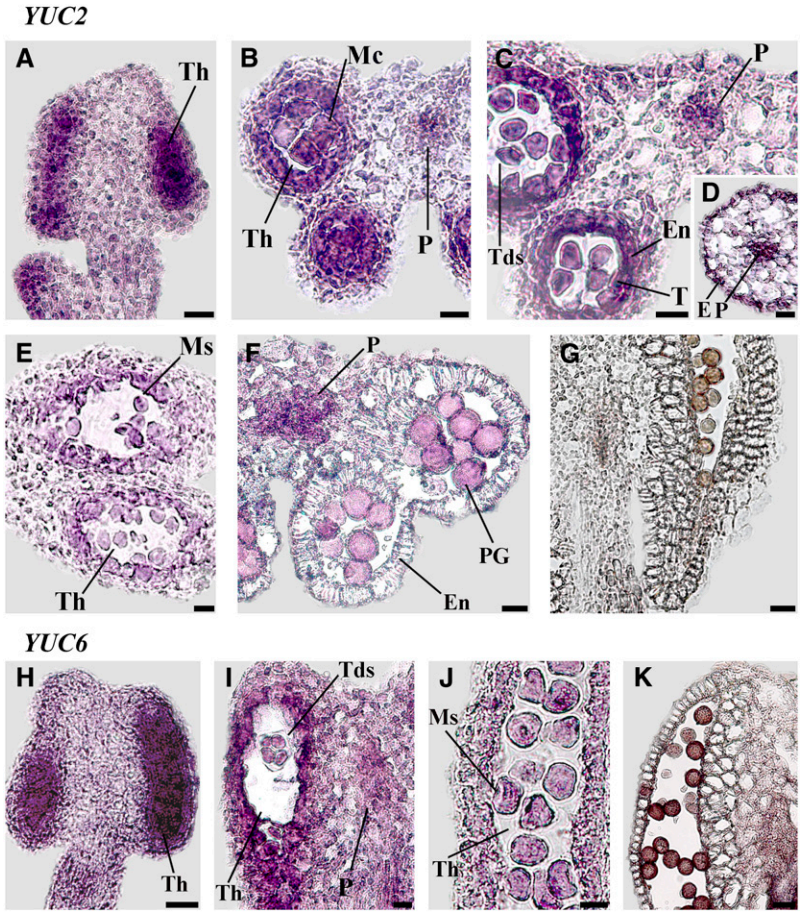

Figure 2. Analysis of the Expression Profiles of *YUC2* and *YUC6* during Stamen Development.

(A) to **(G)** RNA in situ hybridization of *YUC2*. Longitudinal and transverse sections of stamens and anthers.
(A) Stamen at stage 8. A strong signal is present in the theca. Bar = 20 μm.
(B) Anther at early stage 9. A strong signal is present in the tissues surrounding the theca and meiocytes. The signal is also present in the procambium. Bar = 10 μm.
(C) Anther at late stage 9. A strong signal is present in the endothecium, tapetum, tetrads, and in the procambium. Bar = 10 μm.
(D) Upper stamen filament at late stage 9. A signal is present in the procambium and epidermal cells. Bar = 20 μm.
(E) Anther at stage 10. A weak signal is present in the tissues surrounding the theca and in microspores. Bar = 10 μm.
(F) Anther at late stage 11. A signal is present in the procambium, absent in the endothecium, and faint in pollen grains. Bar = 20 μm.
(G) Anther at stage 12. Signal is absent. Bar = 30 μm.
(H) to **(K)** RNA in situ hybridization of *YUC6.*
(H) Stamen at stage 8. A strong signal is present in the theca. Bar = 20 μm.
(I) Anther at late stage 9. A strong signal is present in the tissues surrounding the theca, tetrads, and in the procambium. Bar = 10 μm.
(J) Anther at stage 10. A weak signal is present in the tissues surrounding the theca and microspores. Bar = 10 μm.
(K) Anther at stage 12. Signal is absent. Bar = 20 μm.
Control hybridizations with sense probes for *YUC2* and *YUC6* are shown in Supplemental Figure 2 online. E, epidermal cells; En, endothecium; Mc, meiocytes; Ms, microspores; P, procambium; PG, pollen grains; T, tapetum; Tds, tetrads; Th, theca.

staining was detectable in stamens of any GUS line. In *TIR1:GUS* flowers, GUS activity was observed in anthers starting from stage 11 (Figure 4A2), mainly localized in the junction region between anther and filament, while at stage 13, it was also detectable in the filament (Figure 4A4). In *AFB1:GUS* and *AFB3:GUS* flowers, GUS activity was also observed in anthers starting, respectively, from stages 11 (Figure 4B2) and 10 (Figure 4D2) and in the filaments at stages 12 (Figure 4B4) and 13 (Figure 4D4). In *AFB2:GUS* flowers, GUS activity was detected in anthers and filaments only at stage 13 (Figure 4C4). GUS activity was also detected in pistils, though at different stages of flower development in the different reporter lines. Histological analysis of GUS-stained *AFB3:GUS* anthers showed that GUS activity was localized at stage 10 in the tissues surrounding the theca, in

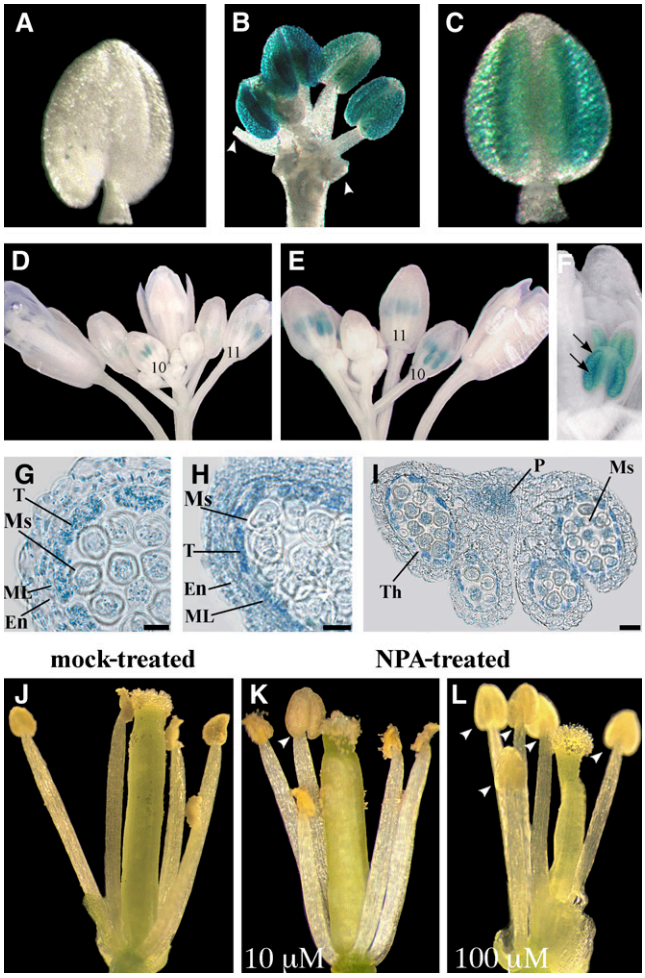

Figure 3. Effects of Blocking Auxin Transport on Auxin Reporter *DR5:GUS* Expression and on Stamen Development.

(A) to **(C)** GUS staining of *DR5:GUS* flower buds and severed anthers cultured in vitro.

(A) Severed anther at time 0. Staining is absent.

(B) Flower bud after 24 h of culture. Strong staining is observed in all anthers. Arrowheads indicate filaments of severed anthers.

(C) Severed anther after 24 h of culture. Strong staining is observed in the whole anther.

(D) to **(F)** Expression of the *DR5:GUS* reporter in flower buds treated with water **(D)** or 10 mM NPA (**[E]** and **[F]**).

(D) Water-treated *DR5:GUS* inflorescence showing GUS staining in anthers at stages 10 and 11. Numbers indicate flower developmental stages.

(E) NPA-treated *DR5:GUS* inflorescence showing GUS staining in anthers of stages late 10 and 11. Numbers indicate flower developmental stages.

(F) Detail of **(E)** NPA-treated *DR5:GUS* inflorescence at late stage 10: GUS signal is observed in the theca and in the tissues surrounding the theca (arrows).

(G) to **(I)** Histochemical analysis of anther transverse sections of *DR5:GUS* flower buds treated with water **(G)** or 100 μM NPA (**[H]** and **[I]**).

(G) Theca of a water-treated anther at late stage 10. GUS staining is observed in tapetum and middle layer cells, in the endothecium, and in microspores. Bar = 10 μm.

(H) Theca of an NPA-treated anther at late stage 10. GUS staining is observed in tapetum and middle layer cells, in the endothecium, and in microspores. Bar = 10 μm.

(I) NPA-treated anther at late stage 11. Intense GUS staining is observed in the theca, in microspores, and in the procambium. Bar = 30 μm.

(J) to **(L)** Phenotype of stamens in mature flowers from *DR5:GUS* inflorescences treated with water **(J)**, 10 μM NPA **(K)**, or 100 μM NPA **(L)**.

(J) Water-treated flower at stage 13. All the anthers are dehiscent.

(K) Flower treated with 10 μM NPA at stage 13. One anther is still indehiscent (arrowhead).

(L) Flower treated with 100 μM NPA at stage 13. All anthers are indehiscent (arrowheads).

En, endothecium; ML, middle layer; Ms, microspores; P, procambium; T, tapetum; Th, theca.

microspores, and barely in the procambium, whereas at stage 12, it was intense in the procambium and very faint in the other tissues (see Supplemental Figure 3 online).

This analysis shows that the *TIR1 AFB* auxin receptor genes are all transcribed, though with somewhat different, but partially overlapping, developmental patterns, in stamens (and pistils) at late developmental stages.

Auxin Perception Mutants Show Precocious Anther Dehiscence and Pollen Maturation

To assess whether auxin is involved in late stamen developmental processes, we analyzed anther dehiscence, pollen maturation, and filament elongation in the auxin perception defective *tir1 afb2 afb3* triple and *tir1 afb1 afb2 afb3* quadruple mutants, which still produce fertile flowers (Dharmasiri et al., 2005). *tir1 afb* mutant flowers were compared with wild-type ones and their stage of development assessed based on well-established developmental and growth markers as described in Methods.

Figure 5A reports the percentage of dehiscent anthers measured in the wild type and *tir1 afb2 afb3* triple and *tir1 afb1 afb2 afb3* quadruple mutant flowers at anthesis (stage 13). In the mutants, anther dehiscence occurred earlier than in wild-type plants and could be observed as early as at stage 10. The effect was more pronounced in quadruple than in triple mutants. Figures 5B to 5D show individual flowers at different stages of development with indehiscent anthers in wild-type and dehiscent anthers in *tir1 afb1 afb2 afb3* quadruple mutant plants.

A comparative histological analysis of anthers from the different plants at different developmental stages was performed. In Figures 5E to 5I, the comparison between wild-type and *tir1 afb1 afb2 afb3* quadruple mutants is reported. In *Arabidopsis*, the anther dehiscence program involves three main sequential steps beginning with the degeneration of the middle layer and tapetum at stage 11 of flower development, when lignification of endothecium cell walls occurs. The second step involves degradation of septum cells leading to a bilocular anther (stage 12), and the third consists of the breakage of stomium cells at stage 13 (Goldberg et al., 1993; Sanders et al., 2000). As shown in Figure 5E, at the end of meiosis (stage 10) before degradation of middle layer and tapetum cells, no lignified thickenings were observed in the endothecium of wild-type anthers, while at the same stage,

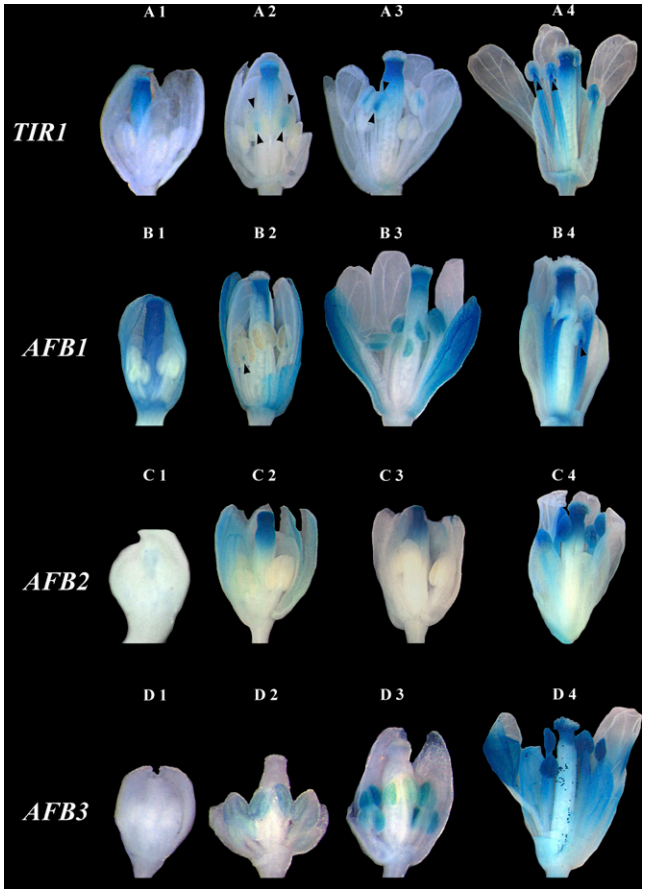

Figure 4. Activity of *TIR1*, *AFB1*, *AFB2*, and *AFB3* Promoters in Developing Stamens and Pistils.

(A) *TIR1:GUS* flower buds at different developmental stages: GUS staining is absent in the stamens and intense in the pistil at late stage 10 **(A1)**. Staining is intense in the junction region between anther and filament (arrowheads), in the vascular tissue of the anthers (arrowheads), and in the apical region of the pistil at stages 11 **(A2)** and 12 **(A3)**. Staining is intense in the anthers and filaments and very intense in the apical region of the filaments (arrowheads) at stage 13 **(A4)**.

(B) *AFB1:GUS* flower buds at different developmental stages: GUS staining is absent in the stamens and intense in the pistil at late stage 10 **(B1)**. Staining is detectable in the junction region between anther and filament (arrowhead) and in the apical region of the pistil at early stage 11 **(B2)**. Staining is intense in the whole anthers and in the apical region of the pistil at stage 11 **(B3)**. Staining is intense in the junction region between anther and filament (arrowhead), in the filaments, and in the apical region of the pistil at stage 12 **(B4)**.

(C) *AFB2:GUS* flower buds at different developmental stages: GUS staining is absent in the stamens and faint in the pistil at stage 9 **(C1)**. Staining is absent in the stamens and intense in the apical region of the pistil at stages 10 **(C2)** and 11 **(C3)**. Staining is strong in the anthers, in the filaments, and in the apical region of the pistil at stage 13 **(C4)**.

(D) *AFB3:GUS* flower buds at different developmental stages: GUS staining is absent at stage 9 **(D1)**. Staining is intense in the anthers at stages 10 **(D2)** and 11 **(D3)**. Staining is strong in the anthers, in the filaments, in pollen grains, and in the apical region of the pistil at stage 13 **(D4)**.

endothecium lignification was clearly visible in *tir1 afb1 afb2 afb3* anthers. These differences in endothecium lignification were also observed later when tapetum degeneration occurred (stage 11): while only initial lignification was observed in wild-type anthers, endothecium lignification was advanced in *tir1 afb1 afb2 afb3* anthers (see Supplemental Figure 4 online).

As shown in Figure 5F, at the end of tapetum degeneration, lysis of the septum took place in both wild-type and *tir1 afb1 afb2 afb3* anthers. However, in wild-type flowers when septum lysis was completed (stage 12), stomium cells were still unbroken (Figures 5G and 5H) and breakage of the stomium took place later at stage 13 (Bowman, 1994). By contrast, in most *tir1 afb1 afb2 afb3* anthers, locules were bent inwards (Figure 5F) and disruption of the septum and of the stomium cells occurred at the same time (Figures 5G and 5I). These results indicate that defective auxin perception results in early anther dehiscence due to a precocious differentiation program compared with the wild type, leading to an early lignification of the walls of endothecium cells; this in turn accounts for the precocious breakage of the stomium.

We then analyzed pollen development to assess whether pollen maturation is altered in *tir1 afb1 afb2 afb3* quadruple mutant anthers and whether it is coupled to anther dehiscence. In *Arabidopsis*, microspores undergo two mitotic divisions inside the theca and are released, at dehiscence, as tricellular pollen grains that germinate upon contact with the stigma (Bowman, 1994). Histological analysis of *tir1 afb1 afb2 afb3* quadruple mutant and wild-type anthers from flower buds at developmental stages between 10 and 13 was performed. At the onset of tapetum degeneration (stage 11), wild-type pollen grains contained only one nucleus (Figure 6A). By contrast, at the same stage most *tir1 afb1 afb2 afb3* pollen grains had already completed the first mitosis, as demonstrated by the presence of two nuclei. Later on, just before septum lysis (late stage 11, Figure 6B), while most pollen grains from wild-type anthers were at the bicellular stage, *tir1 afb1 afb2 afb3* pollen grains had already completed the second mitosis and were at the tricellular stage. As the trinucleate stage is the final step of pollen maturation, these data point to a precocious maturation of pollen grains in *tir1 afb1 afb2 afb3* anthers and suggest that pollen maturation and anther dehiscence are coregulated.

To confirm this, the in vitro germination capacity of pollen grains from *tir1 afb1 afb2 afb3* early-dehiscing anthers at developmental stages 11 and 12 was compared with that of wild-type pollen at the same stages. As shown in Figure 6C, while wild-type pollen grains had not germinated after 24 h of culture, between 30 and 60% of the pollen grains from *tir1 afb1 afb2 afb3* anthers had formed pollen tubes. These results indicate that defective auxin perception results in early-dehiscing anthers releasing precociously matured pollen grains.

Auxin Perception Mutants Have Short Filaments Due to Defective Preanthesis Filament Elongation

To assess whether defective auxin perception affects filament growth also, we measured filament length at different stages of flower development in *tir1 afb1 afb2 afb3* quadruple mutant and wild-type plants. As shown in Figure 7A, *tir1 afb1 afb2 afb3* and

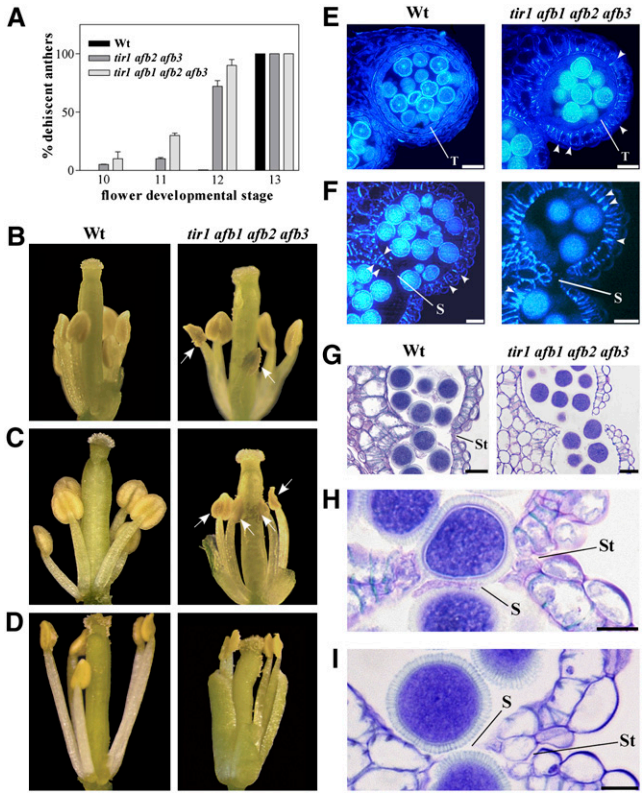

Figure 5. Early Anther Dehiscence Due to Premature Endothecium Lignification in *tir1 afb2 afb3* Triple and *tir1 afb1 afb2 afb3* Quadruple Mutant Flowers.

(A) Percentage of dehiscent anthers in wild-type, *tir1 afb2 afb3*, and *tir1 afb1 afb2 afb3* flowers at different developmental stages. Seven plants of each genotype were analyzed. Means ± SE from 50 flowers are reported.
(B) to **(D)** Wild-type and *tir1 afb1 afb2 afb3* flowers at different stages of development.
(B) Wild-type and *tir1 afb1 afb2 afb3* flowers at stage 11: nondehiscent anthers in wild-type flowers, whereas partially dehiscent anthers are visible in *tir1 afb1 afb2 afb3* flowers (arrows).
(C) Wild-type and *tir1 afb1 afb2 afb3* flowers at stage 12: nondehiscent anthers in wild-type flowers and fully dehiscent anthers are visible in *tir1 afb1 afb2 afb3* flowers (arrows).
(D) Wild-type and *tir1 afb1 afb2 afb3* flowers at stage 13: fully dehiscent anthers are visible in the wild type and in *tir1 afb1 afb2 afb3* flowers.
(E) to **(I)** Histological analysis of wild-type and *tir1 afb1 afb2 afb3* anthers at different developmental stages. Representative transverse sections are shown.
(E) and **(F)** Anthers visualized by fluorescence microscopy.
(E) Wild-type and *tir1 afb1 afb2 afb3* anthers at stage 10: lignification is absent in wild-type endothecium but abundant in the endothecium of *tir1 afb1 afb2 afb3* anthers (arrowheads). Bars = 20 μm.
(F) Wild-type and *tir1 afb1 afb2 afb3* anthers at early stage 12: endothecium lignification is completed in both wild-type and *tir1 afb1 afb2 afb3* anthers (arrowheads). Note the locules bent inwards in the *tir1 afb1 afb2 afb3* anthers. Bars = 20 μm.
(G) to **(I)** Anthers stained with Toluidine blue and visualized under light microscopy.
(G) Wild-type and *tir1 afb1 afb2 afb3* anthers at stage 12: lysis of the septum occurred and stomium cells are unbroken in wild-type anthers, whereas concomitant lysis of the stomium occurred in *tir1 afb1 afb2 afb3* anthers. Bars = 20 μm.
(H) Wild-type anther at early stage 12: detail of the septum region during septum lysis. Stomium cells are unbroken. Bar = 10 μm.
(I) *tir1 afb1 afb2 afb3* anther at early stage 12: detail of the septum region during septum lysis. The locules are bent inwards and stomium cells are parted. Bar = 10 μm.
S, septum; St, stomium; T, tapetum.

wild-type filaments were of comparable length up to stage 10 (at the onset of preanthesis filament elongation), while starting from stage 11, growth of *tir1 afb1 afb2 afb3* filaments was reduced, resulting in filaments ~25% shorter ($P < 0.01$) than the wild type in mature flowers (stage 13).

It should be pointed out that in *tir1 afb1 afb2 afb3* quadruple mutants, no difference in filament length was observed (in any developmental stage) between stamens with dehiscing or nondehiscing anthers, indicating that dehiscence of the anther does not stop the filament from growing.

Interestingly, in mature flowers of *tir1 afb1 afb2 afb3* quadruple mutants, pistils also were ~25% shorter than in the wild type (i.e., 1.78 ± 0.08 SE mm compared with 2.37 ± 0.09 SE mm, $P < 0.01$): this coordinated growth reduction of stamens and pistils allowed the former to reach the latter at anthesis.

Additional phenotypes of *tir1 afb2 afb3* triple and *tir1 afb1 afb2 afb3* quadruple mutant flowers included a reduced number of stamens (Figure 7B) and distorted pistils in 30% of triple and in 60% of quadruple mutant flowers (see Figure 5D).

In the *tir1 afb* auxin perception multiple mutants used in this work, auxin synthesis may still occur but should not result in any effect on the activity of the DR5 promoter due to a defective auxin signal transduction pathway. GFP fluorescence was analyzed in the *tir1 afb2 afb3* triple mutants harboring the *DR5:GFP* construct (*tir1 afb2 afb3 DR5:GFP*) and compared with the fluorescence pattern observed in wild-type *DR5:GFP* flowers. Fluorescence was absent from the tip of the anther and only barely detectable in the apex of the pistil at the tetrad stage in *tir1 afb2 afb3 DR5:GFP* flowers (see Supplemental Figures 5A and 5B online), while it was clearly visible in wild-type *DR5:GFP* flowers (Figures 1O to 1Q). Analogously, GFP fluorescence was not detected in tapetum cells and in the junction region between anther and filament (see Supplemental Figures 5C and 5D online) in the *tir1 afb2 afb3* mutant background, whereas it was observed in wild-type *DR5:GFP* flowers (Figures 1L to 1N). These findings indicate that the *DR5:GFP* reporter construct is not expressed at stages 10 and 11 in *tir1 afb* multiple mutants.

At the same time, the absence of transcription of *TIR1 AFB* receptor genes in stamens at early stages of development explains why the DR5 promoter cannot be induced by exogenous auxin at stages 8 and 9, as shown in Figures 1R to 1U.

Auxin Transport Mutants Have Short Filaments Similar to Auxin Perception Mutants but Only Moderately Affected Anther Dehiscence and Pollen Maturation

Short filaments were also observed in *mdr1 pgp1* double mutants defective in the auxin transporters MDR1 (or PGP19) and

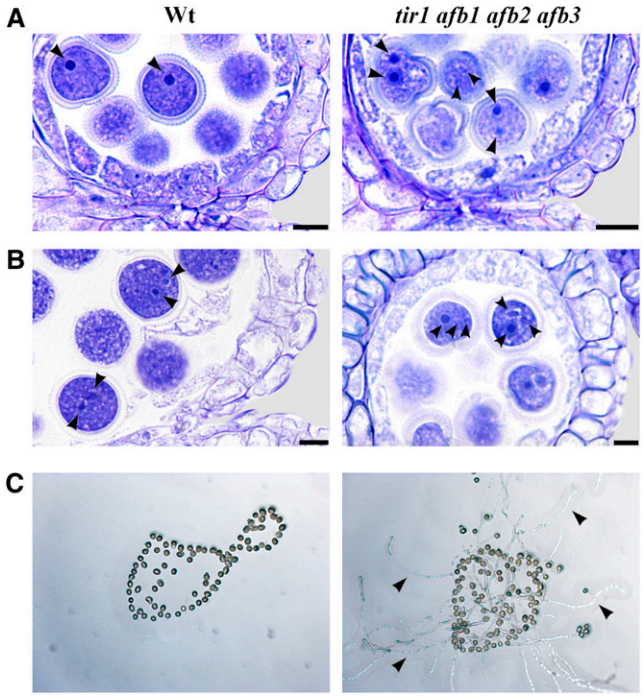

Figure 6. Premature Pollen Maturation in *tir1 afb1 afb2 afb3* Flowers.

(A) and **(B)** Histological analysis of pollen maturation of wild-type and *tir1 afb1 afb2 afb3* anthers at different developmental stages. Anthers were stained with Toluidine blue and visualized in bright field.

(A) Wild-type and *tir1 afb1 afb2 afb3* anthers at early stage 11: one nucleus is observed in pollen grains of wild-type anthers (arrowhead), whereas two nuclei are observed in pollen grains of *tir1 afb1 afb2 afb3* anthers (arrowhead). Bars = 10 μm.

(B) Wild-type and *tir1 afb1 afb2 afb3* anthers at late stage 11: two nuclei (arrowheads) are observed in pollen grains of wild-type anthers, whereas three nuclei (arrowheads) are observed in pollen grains of *tir1 afb1 afb2 afb3* anthers. Bars = 10 μm.

(C) In vitro germination assay of pollen grains from wild-type and *tir1 afb1 afb2 afb3* early-dehiscing anthers. Pollen grains from wild-type non-dehiscent anthers at stage 11 are shown on the left. No pollen tube formation is observed after 24 h of culture. Pollen grains from early-dehiscing anthers of *tir1 afb1 afb2 afb3* flowers at stage 11 are shown on the right. Pollen tube formation (arrowheads) is observed in many pollen grains after 24 h of culture.

PGP1 (Noh et al., 2001). We thus analyzed these double mutants to establish whether they would be defective in the same stages of filament growth as *tir1 afb* multiple mutants and whether they would have an altered timing of anther dehiscence and pollen maturation.

We compared filament lengths of *mdr1 pgp1* double mutant and wild-type flowers at stage 10 (before preanthesis growth begins) and at stage 13 (at the end of preanthesis stamen elongation). While at stage 10 the two types of stamens were of comparable length, at stage 13 stamens of *mdr1 pgp1* double mutants were 20% shorter ($P < 0.01$) than the wild type (Figures 8A and 8B), indicating that the extent of the reduction in length is approximately the same in auxin transport and auxin perception (*tir1 afb*) mutants (cf. with Figure 7A) and that in both cases the defective growth phase is preanthesis growth.

No *mdr1 pgp1* double mutant anthers were dehiscent at stage 11 (compared with ~30% dehiscent anthers of the *tir1 afb1 afb2 afb3* quadruple mutants, as described above), and only ~15% were at stage 12 (as compared with >90% of the *tir1 afb1 afb2 afb3* quadruple mutants and none of the wild-type anthers; see Figure 5A) as exemplified in Figures 8C and 8D. Comparative histological analysis showed that the small percentage of early dehiscent *mdr1 pgp1* double mutant anthers had enhanced lignification (Figures 8E and 8F) leading to early breakage of the stomium (Figure 8G).

Most pollen grains of *mdr1 pgp1* double mutant anthers showed only one nucleus at early stage 11 (Figure 8H), as in the case of normal pollen and in contrast with most *tir1 afb* quadruple mutant pollen grains that already had two nuclei (see above). The final trinucleated state was reached after stage 12 in the pollen grains of most transport mutants (as in the wild type), while only a small percentage (as opposed to the majority in *tir1 afb* multiple mutants) showed precocious maturation at late stage 11 (Figure 8I).

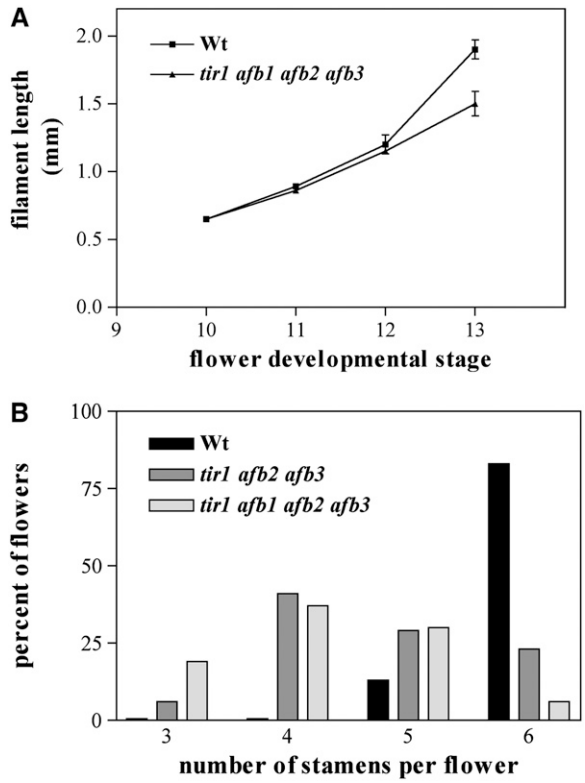

Figure 7. Reduction in Preanthesis Filament Elongation and Number of Stamens in *tir1 afb* Mutant Flowers.

(A) Stamen filament elongation rate in wild-type and *tir1 afb1 afb2 afb3* flowers. Filaments from four wild-type and four mutant plants were analyzed. Bars represent SD from the mean ($n = 12$).

(B) Percentage of flowers with a given stamen number at anthesis in the wild type, *tir1 afb2 afb3*, and *tir1 afb1 afb2 afb3*. One hundred flowers from four plants of each genotype were analyzed.

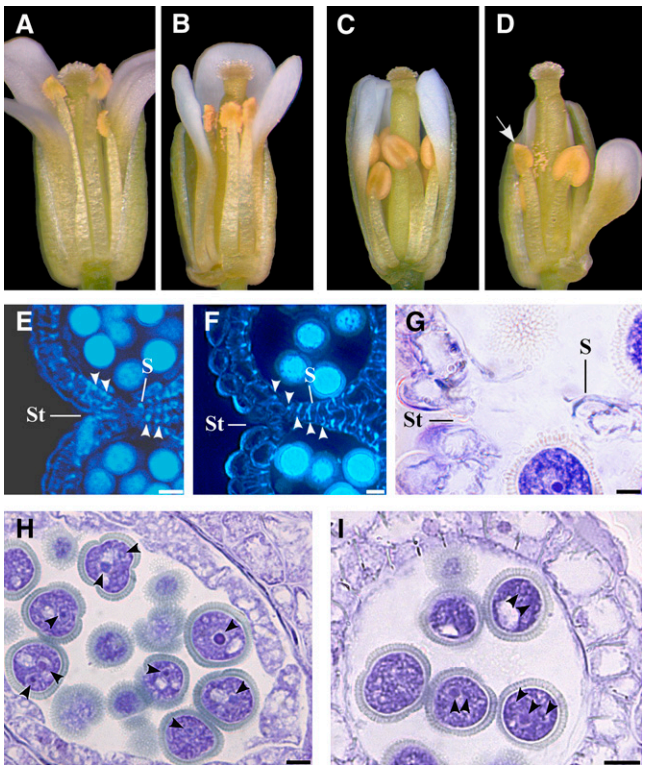

Figure 8. Analysis of Late Stamen Development in *mdr1 pgp1* Mutant Flowers Defective in Auxin Transport.

(A) to **(D)** Wild-type and *mdr1 pgp1* flowers at different stages of development.

(A) and **(B)** Wild-type and *mdr1 pgp1* flowers at stage 13: stamen filaments reached the pistil in the wild-type flower **(A)**, whereas they are shortened in the *mdr1 pgp1* flower **(B)**.

(C) and **(D)** Wild-type and *mdr1 pgp1* flowers at stage 12: nondehiscent anthers in the wild-type flower **(C)** and one dehiscent anther (arrow) in the *mdr1 pgp1* flower **(D)**.

(E) to **(I)** Histological analysis of wild-type and *mdr1 pgp1* anthers at different developmental stages. Representative transverse sections are shown.

(E) and **(F)** Anthers visualized by fluorescence microscopy. Wild-type **(E)** and *mdr1 pgp1* anthers **(F)** at late stage 11. Endothecium lignification (arrowheads) is observed in wild-type anthers, whereas it is increased in *mdr1 pgp1* anthers. Bars = 10 μm.

(G) to **(I)** Anthers were stained with Toluidine blue and visualized under light microscopy.

(G) *mdr1 pgp1* anther at stage 12: detail of the septum region during septum lysis. Stomium cells are parted. Bar = 10 μm.

(H) and **(I)** Hystological analysis of pollen maturation in *mdr1 pgp1* anthers.

(H) *mdr1 pgp1* anther ar early stage 11: one or two nuclei (arrowheads) are observed in pollen grains. Bar = 10 μm.

(I) *mdr1 pgp1* anther at late stage 11: two or three nuclei (arrowheads) are observed in pollen grains. Bar = 10 μm.

S, septum; St, stomium.

Accordingly, pollen grains in the small minority of *mdr1 pgp1* early-dehiscing anthers were able to germinate upon 24 h in vitro culture, while immature pollen grains from indehiscent *mdr1 pgp1* anthers, as in the case of the wild type, were not (see Supplemental Figure 6 online).

DISCUSSION

By means of data on DR5 activity localization, auxin transport, tissue-specific expression of auxin biosynthetic genes, and of phenotypic analysis of mutants defective in auxin perception and in auxin transport, in this article, we point to auxin as a key regulator of the developmental processes occurring late in stamen maturation: anther dehiscence, pollen maturation, and preanthesis filament elongation.

In Anthers, Auxin Biosynthetic Genes and the DR5 Promoter Are Active until the First Steps of Dehiscence, Pollen Maturation, and Filament Elongation Are Completed

Analyzing the activity of the auxin-sensitive DR5 promoter fused with the GUS and GFP reporter genes, we show, in agreement with and considerably extending previous evidence (Aloni et al., 2006; Feng et al., 2006), that DR5 is very active at stage 10 in the tissues surrounding the theca, in microspores and anther-filament procambium, before the onset of anther dehiscence, pollen maturation, and preanthesis filament elongation. After stage 10, DR5 activity decreases and by stage 12, when anthers become bilocular and the first step of anther dehiscence, pollen maturation, and filament elongation is completed, DR5 activity is no longer detectable throughout the stamen. Although DR5 activity does not distinguish between auxin concentration and auxin perception, and responds also to brassinolides, we show here that auxin applied to inflorescences either in planta or in vitro is capable of inducing *DR5:GUS*, as in part reported by Aloni et al. (2006). In particular, we show that exogenous auxin activates *DR5:GUS* activity only (at developmental stages) when the transcripts of the *TIR1*, *AFB1*, *AFB2*, and *AFB3* genes encoding auxin receptors are present but not when they are absent (see below). Moreover, *DR5:GUS* activity is not detectable in *tir1 afb* multiple mutants, where auxin is not perceived. These data suggest that in developing stamens the observed activity of the DR5 promoter reflects the activity of auxin.

We suggest that DR5 activity in the anthers is mainly due to local synthesis of auxin based on three lines of indirect evidence. First, because the *YUC2* and *YUC6* auxin biosynthetic genes are indeed transcribed in anthers, in agreement with evidence shown by Cheng et al. (2006), and, although their transcription does not directly measure auxin biosynthesis, their expression pattern is compatible with the DR5 reporter data. The *YUC* transcripts are abundant in anthers before DR5 activity becomes evident, at premeiotic stage (stage 8) and during meiosis (stage 9), in tissues surrounding the theca, in meiocytes, and in the anther-filament procambium; their level then declines being residually present only in the anther procambium at late stage 11 before the drop in DR5 activity. Second, indirect evidence is that neither blocking transport to *DR5:GUS* anthers in planta at early stages (premeiotic and meiotic) of flower development with the auxin transport

inhibitor NPA nor severing anthers at a premeiotic stage from the flower buds and letting them mature in vitro impaired DR5 activity in anthers. The third line of evidence is the phenotype of *mdr1 pgp1* double mutants impaired in auxin transport (see below).

Auxin Regulates Anther Dehiscence, Pollen Maturation, and Filament Growth

In a previous article, we showed that expression of the oncogene *rolB* causing a local increase of auxin sensitivity in tobacco anthers resulted in delayed anther dehiscence, suggesting an involvement of auxin in this process (Cecchetti et al., 2004). Here, the use of the *tir1 afb* multiple mutant lines enabled us to study the effects of a severe local decrease in auxin perception during late stages of stamen development. Previous data (Cheng et al., 2006) suggested that auxin is necessary in late stamen development: in *yuc2 yuc6* auxin biosynthetic mutants, stamen development is blocked, as no pollen grains are formed and stamen elongation does not occur, leading to sterile flowers. Stamen development in these mutants could be rescued by expression of the bacterial auxin biosynthesis gene iaaM under the control of *YUC6* promoter (Cheng et al., 2006). However, the use of the *yuc2 yuc6* mutants did not allow the study of the effect of auxin on the individual processes analyzed in this work.

The *tir1 afb* multiple mutant lines used here are most suitable for this analysis because, though defective in auxin perception, they are still able to form fertile flowers (Dharmasiri et al., 2005). We show that *TIR1*, *AFB1*, *AFB2*, and *AFB3* genes encoding auxin receptors are transcribed in the tissues involved in late stamen development when DR5 activity is observed. We show that loss of TIR1 AFB function in the *tir1 afb* multiple mutants causes early anther dehiscence and pollen maturation and reduced stamen filament length.

We also show that in *tir1 afb* mutant stamens, the auxin-induced DR5 promoter is not active. In agreement, exogenous auxin in the wild-type background can activate the DR5 promoter (as discussed above) at late developmental stages (12 and 13) when the *TIR1*, *AFB1*, *AFB2*, and *AFB3* are transcribed, while it cannot at earlier stages (8 and 9) when *TIR1* and *AFB* transcripts are absent, indicating that the effect of auxin on the late developmental processes of the stamen is mediated by the TIR1 AFB receptors.

We show that the *TIR1*, *AFB1*, *AFB2*, and *AFB3* transcripts have discrete but partially overlapping localizations in the stamen. This may reflect distinct developmental functions during stamen maturation and suggests that these auxin receptors act partially redundantly in perceiving auxin in the *Arabidopsis* stamen, as previously shown in roots by Dharmasiri et al. (2005). However, a more accurate analysis would be necessary to demonstrate specific roles for the TIR1 AFB receptors, since the limits of our reporter line data include not taking into account possible posttranscriptional regulations, such as the effects of microRNAs (Navarro et al., 2006).

Early Anther Dehiscence Is Due to Premature Endothecium Lignification

In *Arabidopsis*, anther dehiscence involves three main sequential steps: degeneration of the middle layer and tapetum, concomitant with endothecium cell wall lignification; septum cell degradation; and breakage of stomium cells (Goldberg et al., 1993; Sanders et al., 1999).

Secondary thickening of the endothecium is essential to allow stomium breakage (Keijzer, 1987; Bonner and Dickinson, 1989; Mitsuda et al., 2005; Mizuno et al., 2007). In this article, we demonstrate that in *tir1 afb* multiple mutants, endothecium lignification occurs earlier than in the wild type and starts before tapetum degeneration (stage 11). Thus, while in wild-type anthers stomium opening follows septum degeneration, in *tir1 afb* multiple mutants, breakage of the septum and of the stomium occurs at the same time as a consequence of premature endothecium lignification.

Our data confirm that stomium breakage depends on endothecium lignification. In agreement, the loss of the transcription factor *MYB26* results in indehiscent anthers by preventing endothecium lignification and stomium breakage (Yang et al., 2007). The secondary thickening of the endothecial cell wall has been described in detail (Dawson et al., 1999; Yang et al., 2007) and involves primarily lignification of cellulose microfibrils. Several genes involved in cellulose remodeling in *Arabidopsis* are regulated by auxin (Osato et al., 2006); thus, we cannot exclude that the early lignification we observed here in auxin perception mutants could be due to a premature deposition of cellulose microfibrils.

Pollen Maturation and Anther Dehiscence Are Coordinated

In *Arabidopsis*, microspores undergo two mitotic divisions: the first starting during tapetum degeneration (stage 11) and the second starting when endothecium lignification is completed (late stage 11) (Kim et al., 2001; Figure 9). Pollen maturation leads to tricellular pollen grains that are capable of germinating. We show here that early dehiscent anthers (stages 11 and 12) of *tir1 afb* multiple mutants contain early maturing trinucleate pollen grains that are able to germinate in vitro, while at the same stages wild-type pollen grains cannot. Early maturation of pollen grains in auxin reception mutants is due to the fact that the two pollen mitotic divisions occur earlier than in the wild type (i.e., before tapetum degeneration and endothecium lignification, respectively).

Thus, in pollen, auxin regulates entry into the cell cycle, confirming previous observations that this hormone regulates genes involved in cell cycle entry and duration (Dewitte and Murray, 2003; Magyar et al., 2005; David et al., 2007; Francis., 2007).

We show that a defect in auxin perception causes synchronously premature anther dehiscence and pollen maturation, suggesting that this hormone coordinates the timing of the two processes. In agreement with our conclusions, indehiscent anthers of the *myb26* mutant mentioned above contain aborted pollen (Yang et al., 2007), and mutation of the Leu-rich repeat receptor-like kinase gene *RPK2* impairs both anther dehiscence and pollen maturation (Mizuno et al., 2007).

It has been shown that JA is involved in anther dehiscence and pollen maturation, as mutants defective in JA synthesis are sterile and show delayed anther dehiscence and reduced pollen germination (Sanders et al., 2000; Stintzi and Browse, 2000; Ishiguro et al., 2001). Exogenous JA rescued these phenotypes and restored fertility only when applied to flower buds at stage

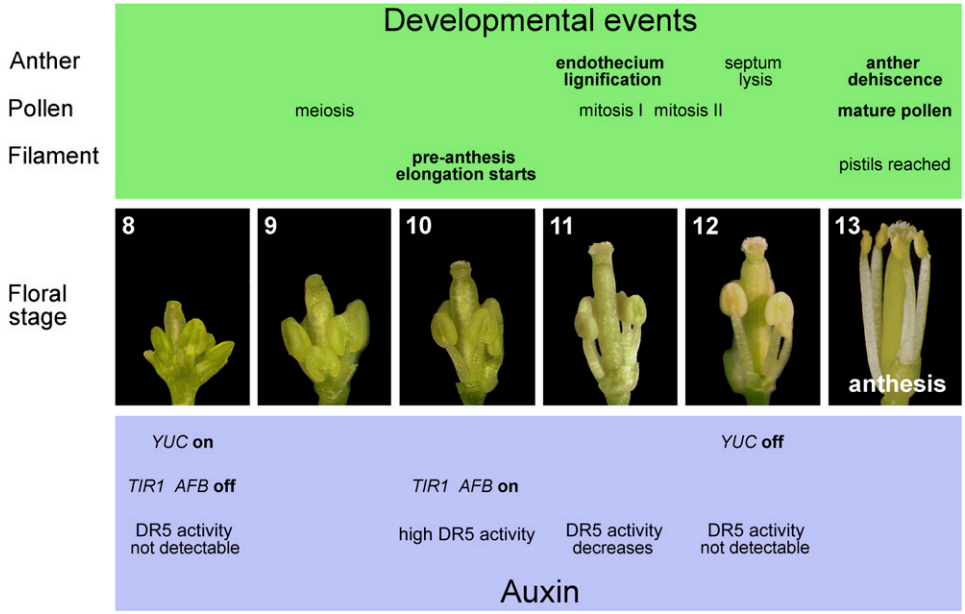

Figure 9. Landmarks in Late Stamen Development.

Main events in the development of anther, pollen, and filament (green panel) and events related to auxin (blue panel), occurring in stamens during late flower development (central panels), as inferred from our data, from stages 8 to 13 (according to Bowman, 1994).

12, when the second pollen mitosis occurs (Stintzi and Browse, 2000); accordingly, the peak of JA production in flowers takes place at stages 11 and 12 (Nagpal et al., 2005). These data point to a role of JA in the final stages of anther dehiscence and pollen maturation, while we show here that auxin acts on the initial stages of these processes. We can hypothesize that in anther and pollen maturation auxin acts on (the levels of) JA. Accordingly, in the double mutants defective in the ARF6 and ARF8 auxin transcription factors, the level of JA is below the detection threshold at all floral stages, and indehiscent *arf6 arf8* anthers dehisce when treated with JA (Nagpal et al., 2005).

Filament Growth Is Uncoupled from Anther Dehiscence but Coupled with Pistil Growth

In *Arabidopsis*, the filament and anther regions become distinguishable at stage 7 of flower development. Subsequently, a first phase of filament elongation occurring from stages 7 to 9 leads to a filament ~0.5 to 1 mm in length. A second growth phase, denominated preanthesis growth, takes place from stage 10 to anthesis and is particularly rapid from stages 12 to 13 (Bowman, 1994; Figure 9). In *tir1 afb* multiple mutants, the first phase of filament growth was normal, but preanthesis growth was slower, resulting in shortened filaments. Analysis of *tir1 afb* GUS lines shows that in filaments at early stages of preanthesis growth (stages 10 to 12), expression of these auxin receptor genes is restricted to the junction region between anther and filament, where DR5 activity is first observed. This suggests that, to promote preanthesis filament growth, auxin first acts in the anther-filament junction. Accordingly, we had previously shown that the junction region plays a key role in tobacco filament growth (Cecchetti et al., 2007).

In *tir1 afb* multiple mutants, filament elongation, though reduced, did not stop upon early anther dehiscence, indicating that the two processes of filament growth and anther dehiscence are uncoupled. At anthesis, the short stamens of the *tir1 afb* multiple mutants reached the level of the stigma because a concurrent reduction in pistil elongation occurred, suggesting a coordinated positive regulation by auxin on stamen filament and pistil growth.

The Phenotype of Auxin Transport Mutants Confirms the Role of Auxin in Late Stages of Stamen Maturation

The proposed role of auxin in filament elongation is in agreement with the short filaments of the *mdr1 pgp1* double mutants impaired in auxin transport (Noh et al., 2001). We show here that the filaments of this double mutant are approximately as short as the ones of the *tir1 afb* multiple mutants and that both types of stamens are impaired in preanthesis growth.

Further analysis of *mdr1 pgp1* mutant stamens shows that they are only moderately affected in the timing of anther dehiscence and pollen maturation and that the alterations observed in a small percentage of *mdr1 pgp1* anthers and pollen grains are qualitatively of the same nature of those of the *tir1 afb* multiple mutants. This confirms that anther dehiscence and pollen maturation are coordinated with each other but independent of filament growth. The anther/pollen phenotype of *mdr1 pgp1* mutant stamens also provides support to the suggestion that transport of auxin from the filament to the anther does not play a major role in the observed activity of the DR5 promoter (i.e., that

the role of auxin in late anther developmental stages is largely played by auxin synthesized in anther tissues).

Auxin transport from the anther to the filament may occur and be developmentally relevant for filament elongation. In fact, NPA-treated flowers showed shorter filaments only if treated at relatively late stages when, as judged from DR5 activity, auxin has already built up in anthers mostly because of local synthesis, suggesting that auxin transported from the anther to the filament late in stamen development may play a role in filament elongation. In this perspective, the slight delay in anther dehiscence observed in NPA-treated flowers may be accounted for by effects of NPA other than on auxin transport (Dhonukshe et al., 2008).

Transport of auxin from the anther to the filament may also explain why the filaments of *mdr1 pgp1* mutant stamens are affected only in preanthesis growth, although further work is needed to assess this point.

In summary, as represented in Figure 9, we suggest that in *Arabidopsis* at the end of meiosis when auxin receptor genes are turned on and auxin biosynthetic genes are still active, auxin triggers stamen elongation and prevents premature anther dehiscence and pollen maturation. Subsequently, the decrease of auxin biosynthetic genes activity and/or changes in auxin sensitivity in tissues involved in anther dehiscence and pollen maturation, trigger these processes.

METHODS

Plant Materials and Treatments

Arabidopsis thaliana mutant lines *tir1 afb2 afb3* and *tir1 afb1 afb2 afb3* (Dharmasiri et al., 2005), kindly provided by Mark Estelle (Indiana University, IN), and *mdr1 pgp1* (Noh et al., 2001), kindly provided by Angus Murphy (Purdue University, IN) and Edgar Spalding (University of Wisconsin, WI), are in the Wassilewskija ecotype and were compared with Wassilewskija wild type. All other lines used in this study were in the Columbia (Col-0) ecotype and were compared with Col-0 wild type. *TIR1:GUS*, *AFB1:GUS*, *AFB2:GUS*, and *AFB3:GUS* (Dharmasiri et al., 2005) were provided by Mark Estelle, *DR5:GUS* (Ulmasov et al., 1997) was provided by Tom Guilfoyle (University of Missouri, MO), and *DR5:GFP* (Blilou et al., 2005) was provided by Jian Xu (Utrecht University, The Netherlands). *tir1 afb2 afb3 DR5:GFP* lines, provided by Mark Estelle, were compared with *DR5:GFP* lines. Plants were grown in a 16-h-light/8-h-dark cycle at 24/21°C until flowering (~4 weeks).

The developmental stages of the flowers of the *tir1 afb2 afb3* triple and *tir1 afb1 afb2 afb3* quadruple mutants and of the *mdr1 pgp1* double mutants were assessed by comparing with wild-type flowers the following developmental and growth markers (Bowman, 1994): (1) stages 8 and 9, floral bud green appearance and absence of stigmatic papillae differentiation; (2) stage 9, meiosis leading to tetrad formation, established by squeezing anthers with acetic orcein solution (Cecchetti et al., 2004), and tapetum presence; (3) stage 10, floral bud green appearance, onset of stigmatic papillae elongation, microspores separated from each other and undegenerated tapetum; (4) stage 11, white petals visible, macroscopic appearance of stigmatic papillae, and tapetum degeneration; (5) stage 12, petals protruding past sepals, septum degeneration in the anther and fully differentiated papillae; (6) stage 13, flower opening with petals bent outwards, stamens that have reached the pistil.

In planta NAA-treatments were performed by spraying 50 μM NAA (Sigma-Aldrich) or water on four inflorescences of two different plants in the morning at 9 AM and spraying again at 4 PM. Twenty-four hours after the first spraying, plants were rinsed with distilled water and inflorescences were collected for GUS staining. In vitro, NAA treatments were performed by incubating eight excised inflorescences in 50 μM NAA or in water for 16 h as described by Ulmasov et al. (1997). Inflorescences were then stained and analyzed for GUS activity. In planta and in vitro experiments were repeated three times.

In planta NPA treatments were performed as described by Nemhauser et al. (2000). *DR5:GUS* plants were sprayed with 10 or 100 μM NPA (Duchefa) with 0.01% Silwet L-77 in the morning at 9 AM and sprayed again at 4 PM. The following day at 9 AM, plants were rinsed with distilled water. Mock treatments were performed with distilled water containing 0.01% Silwet L-77. Flowers were collected, 24 h after the first spraying, at stages 10 or 11, directly for GUS analysis or phenotypically analyzed, 24, 48, 72, and 96 h after the first spraying, at stages 11 to 13. Experiments were performed five times on 10 different plants.

Fifteen floral buds at stage 8 of development were dissected from *DR5:GUS* inflorescences and two anthers from each bud severed. One anther was analyzed for GUS staining at the excision time and the other was cultured, together with the flower bud, on half-strength agar Murashige and Skoog medium. After 24 h, microsporogenesis stage was determined by acetic orcein solution (see above) and GUS staining performed (see below).

GFP and GUS Analysis

DR5:GFP and *tir1 afb2 afb3 DR5:GFP* flower buds were collected, stamen and pistils were isolated, and hand-cut sections mounted in Acquovitrex (Carlo Erba). GFP fluorescence was monitored with a Leica DMRB fluorescence microscope equipped with a DC 500 digital camera. Fluorescence was excited with a fluorescein isothiocyanate filter set (excitation band-pass 450 to 490, dichroic RKP 510, emission long-pass 515). Specific fluorescence was confirmed with a double wavelength filter set (band-pass 490/20 and band-pass 575/30), dichroic filters RKPs 505 and 600, and emission filter band-passes 525/20 and 635/40. Images were collected by a Leica IM 1000 imaging system. *DR5:GUS*, *TIR1:GUS*, *AFB1:GUS*, *AFB2:GUS*, and *AFB3:GUS* inflorescences were collected and GUS analysis was performed as previously described (Cecchetti et al., 2004).

Images were acquired by a stereomicroscope equipped with a DC 500 digital camera. Microscopic sections were prepared from GUS-stained flower buds as described below and 10-μm sections photographed as described below.

Statistical Analysis

Differences between the means in stamen and pistil lengths were statistically analyzed as previously described (Cecchetti et al., 2007).

Histological and Cytological Analysis

Floral buds were embedded in Technovit 7100 (Kulzer), and 3-μm sections were stained with 1% Toluidine blue. Images were acquired by a DC 500 digital camera applied to a DMRB microscope (Leica).

Lignin autoflorescence was examined using the following filter combination: excitation filter 340 to 380 nm, bichromatic beam splitter 400 nm, and barrier filter 425 nm.

For the in vitro pollen germination assay shown in Figure 6, pollen grains were extracted from six wild-type indehiscent anthers at stage 11, six wild-type indehiscent anthers at stage 12, six *tir1 afb1 afb2 afb3* dehiscent anthers at stage 11, and six dehiscent anthers at stage 12. For the in vitro germination assay shown in Supplemental Figure 6 online, pollen grains were extracted from six wild-type indehiscent anthers at stage 12, six *mdr1 pgp1* dehiscent anthers at stage 12, and six indehiscent anthers at stage 12. Pollen grains were incubated for 24 h on agarized medium containing 100 g/L sucrose and 0.025 H_3BO_3, pH 6.5.

Pollen tube formation was monitored under light microscopy. Images were acquired as described above.

In Situ Hybridization

RNA was extracted from wild-type Col-0 flower buds and reverse transcribed as previously described (Cecchetti et al., 2007). cDNA was amplified using the following primers: yuc2 (5′-CAATTCTTGAGA-GATTTTCTTAT-3′ and 5′-TCATTAAGCACCTAGTTTCC-3′) and yuc6 (5′-ACACTCTCATCAAAACACAAA-3′ and 5′-GTGACGACGCAGATA-CGA-3′).

The partial *yuc2* and *yuc6* cDNA fragments were cloned into the vector pGEM using the cloning kit pGEM-T Easy Vector (Promega) and verified by sequencing. Digoxigenin-labeled RNA probes were synthesized by in vitro transcription using the DIG RNA labeling kit (Roche).

In situ analysis was performed as previously described (Cecchetti et al., 2007). Hybridizations with sense probes of *YUC2* and *YUC6* genes are shown in Supplemental Figure 2 online.

Accession numbers

Sequence data from this article can be found in the Arabidopsis Genome Initiative or GenBank/EMBL databases under the following accession numbers: NM_116163 (*TIR1*), NM_116555 (*AFB1*), NM_113593 (*AFB2*), NM_101152 (*AFB3*), NM_117399 (*YUC2*), NM_122473 (*YUC6*), NP_181228 (*PGP1*), and NM_113807 (*MDR1*).

Supplemental Data

The following materials are available in the online version of this article.

Supplemental Figure 1. Expression of the *DR5:GUS* Reporter after Water Treatment of in Planta or Excised Inflorescences.

Supplemental Figure 2. RNA in Situ Hybridizations Using Sense Probes of *YUC* Genes.

Supplemental Figure 3. Histochemical Analysis of Transverse Sections of *AFB3:GUS* Anthers at Stages 10 and 12 of Development.

Supplemental Figure 4. Transverse Sections of Wild-Type and *tir1 afb1 afb2 afb3* Anthers at Stage 11 of Development, Visualized by Fluorescence Microscopy.

Supplemental Figure 5. Fluorescence Images of Anthers and Pistils at Different Developmental Stages from *tir1 afb2 afb3* Expressing the *DR5:GFP* Auxin-Responsive Reporter.

Supplemental Figure 6. In Vitro Germination Assay of Pollen Grains from *mdr1 pgp1* Indehiscent and Early-Dehiscing Anthers.

ACKNOWLEDGMENTS

We thank Mark Estelle for kindly providing *tir1 afb* multiple mutants, *TIR1 AFB* promoter:GUS fusions, and *DR5:GFP* in *tir1 afb* multiple mutants, Sabrina Sabatini for critical reading of the manuscript, and Giovanna Serino for helpful discussions. This work was partially supported by research grants from the Ministero dell'Istruzione, dell'Università e della Ricerca, Fondo per gli Investimenti della Ricerca di Base, Networking the European Research Area, Plant Genomics to P.C. and the Ministero dell'Istruzione, dell'Università e della Ricerca, Progetti di Ricerca di Interesse Nazionale to M.C. and P.C. and a grant from Università La Sapienza (Progetto di Ateneo) to M.M.A.

Received December 17, 2007; revised June 27, 2008; accepted July 2, 2008; published July 15, 2008.

REFERENCES

Aloni, R., Langhans, M., Aloni, E., and Ullrich, C.I. (2006). Role of auxin in regulating *Arabidopsis* flower development. Planta **223:** 315–328.

Blilou, I., Xu, J., Wildwater, M., Willemsen, V., Paponov, I., Friml, J., Heidstra, R., Aida, M., Palme, K., and Scheres, B. (2005). The PIN auxin efflux facilitator network controls growth and patterning in *Arabidopsis* roots. Nature **433:** 39–44.

Bonner, L.J., and Dickinson, H.G. (1989). Anther dehiscence in *Lycopersicon esculentum* Mill. I. Structural aspects. New Phytol. **113:** 97–115.

Bowman, J. (1994). Arabidopsis: An Atlas of Morphology and Development. (New York: Springer-Verlag).

Cecchetti, V., Altamura, M.M., Serino, G., Falasca, G., Costantino, P., and Cardarelli, M. (2007). *ROX1*, a gene induced by *rolB*, is involved in procambial cell proliferation and xylem differentiation in tobacco stamen. Plant J. **49:** 27–37.

Cecchetti, V., Pomponi, M., Altamura, M.M., Pezzotti, M., Marsilio, S., D'Angeli, S., Tornielli, G.B., Costantino, P., and Cardarelli, M. (2004). Expression of *rolB* in tobacco flowers affects the coordinated processes of anther dehiscence and style elongation. Plant J. **38:** 512–525.

Cheng, Y., Dai, X., and Zhao, Y. (2006). Auxin biosynthesis by the YUCCA flavin monooxygenases controls the formation of floral organs and vascular tissues in *Arabidopsis.* Genes Dev. **20:** 1790–1799.

David, K.M., Couch, D., Braun, N., Brown, S., Grosclaude, J., and Perrot-Rechenmann, C. (2007). The auxin-binding protein 1 is essential for the control of cell cycle. Plant J. **50:** 197–206.

Dawson, J., Sozen, E., Vizir, I., VanWaeyenberge, S., Wilson, Z.A., and Mulligan, B.J. (1999). Characterization and genetic mapping of a mutation (*ms35*) which prevents anther dehiscence in *Arabidopsis thaliana* by affecting secondary wall thickening in the endothecium. New Phytol. **144:** 213–222.

Dewitte, W., and Murray, J.A. (2003). The plant cell cycle. Annu. Rev. Plant Biol. **54:** 235–264.

Dharmasiri, N., Dharmasiri, S., Weijers, D., Lechner, E., Yamada, M., Hobbie, L., Ehrismann, J.S., Jürgens, G., and Estelle, M. (2005). Plant development is regulated by a family of auxin receptor F-box proteins. Dev. Cell **9:** 109–119.

Dhonukshe, P., et al. (2008). Auxin transport inhibitors impair vesicle motility and actin cytoskeleton dynamics in diverse eukaryotes. Proc. Natl. Acad. Sci. USA **105:** 4489–4494.

Feng, X.L., Ni, W.M., Elge, S., Mueller-Roeber, B., Xu, Z.H., and Xue, H.W. (2006). Auxin flow in anther filaments is critical for pollen grain development through regulating pollen mitosis. Plant Mol. Biol. **61:** 215–226.

Francis, D. (2007). The plant cell cycle - 15 years on. New Phytol. **174:** 261–278.

Goldberg, R.B., Beals, T.P., and Sanders, P.M. (1993). Anther development: Basic principles and practical applications. Plant Cell **5:** 1217–1229.

Ishiguro, S., Kawai-Oda, A., Ueda, J., Nishida, I., and Okada, K. (2001). The DEFECTIVE IN ANTHER DEHISCENCE gene encodes a novel phospholipase A1 catalyzing the initial step of jasmonic acid biosynthesis, which synchronizes pollen maturation, anther dehiscence, and flower opening in Arabidopsis. Plant Cell **13:** 2191–2209.

Keijzer, C.J. (1987). The processes of anther dehiscence and pollen dispersal. II. The formation and the transfer mechanism of pollenkitt, cell-wall development of the loculus tissues and a function of orbicules in pollen dispersal. New Phytol. **105:** 499–507.

Kim, S.Y., Hong, C.B., and Lee, I. (2001). Heat shock stress causes stage specific male sterility in *Arabidopsis thaliana*. J. Plant Res. **114:** 301–307.

Magyar, Z., De Veylder, L., Atanassova, A., Bakó, L., Inzé, D., and Bögre, L. (2005). The role of the *Arabidopsis* E2FB transcription factor in regulating auxin-dependent cell division. Plant Cell **17:** 2527–2541.

Mitsuda, N., Seki, M., Shinozaki, K., and Ohme-Takagi, M. (2005). The NAC transcription factors NST1 and NST2 of *Arabidopsis* regulate secondary wall thickenings and are required for anther dehiscence. Plant Cell **17:** 2993–3006.

Mizuno, S., Osakabe, Y., Maruyama, K., Ito, T., Osakabe, K., Sato, T., Shinozaki, K., and Yamaguchi-Shinozaki, K. (2007). Receptor-like protein kinase 2 (RPK 2) is a novel factor controlling anther development in *Arabidopsis thaliana*. Plant J. **50:** 751–766.

Nagpal, P., Ellis, C.M., Weber, H., Ploense, S.E., Barkawi, L.S., Guilfoyle, T.J., Hagen, G., Alonso, J.M., Cohen, J.D., Farmer, E.E., Ecker, J.R., and Reed, J.W. (2005). Auxin response factors ARF6 and ARF8 promote jasmonic acid production and flower maturation. Development **132:** 4107–4118.

Navarro, L., Dunoyer, P., Jay, F., Arnold, B., Dharmasiri, N., Estelle, M., Voinnet, O., and Jones, J.D.G. (2006). A plant miRNA contributes to antibacterial resistance by repressing auxin signaling. Science **312:** 436–439.

Nemhauser, J.L., Feldman, L.J., and Zambryski, P.C. (2000). Auxin and *ETTIN* in *Arabidopsis* gynoecium morphogenesis. Development **127:** 3877–3888.

Noh, B., Murphy, A.S., and Spalding, E.P. (2001). Multidrug resistance-like genes of Arabidopsis required for auxin transport and auxin-mediated development. Plant Cell **13:** 2441–2454.

Okada, K., Ueda, J., Komaki, M.K., Bell, C.J., and Shimura, Y. (1991). Requirement of the auxin polar transport system in early stages of Arabidopsis floral bud formation. Plant Cell **3:** 677–684.

Osato, Y., Yokoyama, R., and Nishitani, K. (2006). A principal role for AtXTH18 in *Arabidopsis thaliana* root growth: A functional analysis using RNAi plants. J. Plant Res. **119:** 153–162.

Ru, P., Xu, L., Ma, H., and Huang, H. (2006). Plant fertility defects induced by the enhanced expression of microRNA167. Cell Res. **16:** 457–465.

Sanders, P.M., Bui, A.Q., Weterings, K., McIntire, K.N., Hsu, Y.C., Lee, P.Y., Truong, M.T., Beals, T.P., and Goldberg, R.B. (1999). Anther development defects in *Arabidopsis thaliana* male-sterile mutants. Sex. Plant Reprod. **11:** 297–322.

Sanders, P.M., Lee, P.Y., Biesgen, C., Boone, J.D., Beals, T.P., Weiler, E.W., and Goldberg, R.B. (2000). The Arabidopsis *DELAYED DEHISCENCE1* gene encodes an enzyme in the jasmonic acid synthesis pathway. Plant Cell **12:** 1041–1061.

Stintzi, A., and Browse, J. (2000). The Arabidopsis male-sterile mutant, opr3, lacks the 12-oxophytodienoic acid reductase required for jasmonate synthesis. Proc. Natl. Acad. Sci. USA **97:** 10625–10630.

Ulmasov, T., Murfett, J., Hagen, G., and Guilfoyle, T.J. (1997). Aux/IAA proteins repress expression of reporter genes containing natural and highly active synthetic auxin response elements. Plant Cell **9:** 1963–1971.

Yang, C., Xu, Z., Song, J., Conner, K., Vizcay Barrena, G., and Wilson, Z.A. (2007). *Arabidopsis MYB26/MALE STERILE35* regulates secondary thickening in the endothecium and is essential for anther dehiscence. Plant Cell **19:** 534–548.

Yassuor, H., Abu-Abied, M., Belausov, E., Madmony, A., Sadot, E., Riov, J., and Rubin, B. (2006). Glyphosate-induced anther indehiscence in cotton is partially temperature dependent and involves cytoskeleton and secondary wall modifications and auxin accumulation. Plant Physiol. **141:** 1306–1315.

Wu, M.F., Tian, Q., and Reed, J.W. (2006). *Arabidopsis microRNA167* controls patterns of *ARF6* and *ARF8* expression, and regulates both female and male reproduction. Development **133:** 4211–4218.